1312
doi:10.1017/S1431927622005396
Microsc. Microanal. 28 (Suppl 1), 2022

(Cryo-) Electron Microscopy Workflows of Interactions between Airborne Pollution Particles and Nasal Epithelial Cells

Victoria Garcia Giner[1*], Sharon Mumby[2], Ramzi Lakhdar[2], Ian Mudway[3], Fan Chung[2], Ian Adcock[2], Alexandra Porter[1]

[1.] Faculty of Engineering, Department of Materials, Imperial College London, London, United Kingdom
[2.] Faculty of Medicine, National Heart & Lung Institute, Imperial College London, United Kingdom
[3] Faculty of Medicine, School of Public Health, Imperial College London, United Kingdom
* Corresponding author: mvg1617@ic.ac.uk

There is a rising concern about the increase in respiratory diseases associated with high levels of air particulate matter (PM) in congested cities. Micro-sized airborne particles, PM 2.5 (<2.5µm) or smaller, which have different compositions and structures, are the most concerning, as they can penetrate through the lung inducing a variety of chronic diseases. PM 2.5 airborne pollution, which includes carbonaceous particles, as well as, redox-active metals, such as Cr, Fe or Ti, can generate cell-damaging free radicals and therefore inflammatory responses and toxicity. Still, it is unknown whether the PM is internalised, and which routes of cell internalisation do these pollutants follow inside respiratory system cells.

In this study, we used electron and ion beam microscopy techniques to analyse the intracellular location and composition of PM 2.5, collected from London Underground and roadside locations, in cell cultures of respiratory system epithelial cells**.** This study also developed workflows that involved complementary imaging and analytical techniques, under cryogenic conditions, for more rapid data acquisition, and less artefactual data, which can be generated using standard room temperature biological sample preparation techniques, that use resins or fixatives. By imaging under cryogenic conditions, EDS compositional analysis of the PM in the cellular environment was possible, without altering their chemical composition. Vitrification of the samples also prevented shrinkage and deformation of the cell morphology. TEM imaging of resin embedded sections of the same cell monolayers was also employed as a benchmark to compare the efficiency of the method described and study the damage to intracellular organelles induced by the PM.

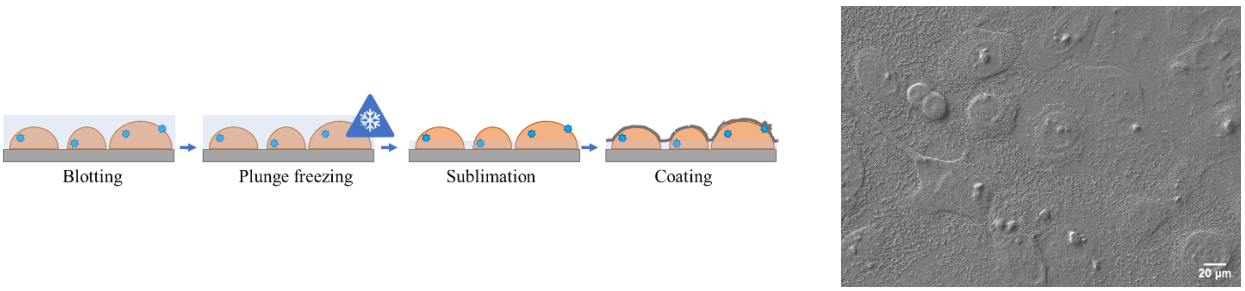

Figure 1. From left to right. Sample preparation workflow for cryo-SEM imaging of cell monolayers. Cryo-SEM imaging of nasal epithelial cells exposed to PM2.5 roadside pollution (Zeiss Auriga Cross beam, SE, 2kV) Exposure of cell monolayer after sublimation of the ice layer, pollution agglomerates can be observed on the surface of the cells (scale bar 20 µm).

Firstly, cryo-scanning electron microscopy (cryo-SEM) protocols were optimised to image the interaction of roadside PM with primary nasal epithelial cells. After the cell monolayer had been

exposed by sublimation of an ice layer, the morphology of the cells became visible, and the pollution PM agglomerates could be observed on the surface [1]. The PM surrounding, and on the surface of the cells, was composed of several metals including Al, Fe, Ti, Si, etc. - and carbonaceous particles (Figure 1). Ga^+ beam cross-sectional milling (Ga-FIB-SEM) of the cryogenic samples was attempted, but the volume removal capabilities of the beam proved insufficient for the micrometric dimensions of the cells. To overcome this challenge, plasma FIB-SEM of embedded cell monolayers exposed to underground pollution was performed to characterise the chemistry and size of particles internalised by the nasal epithelial cells. Xe and O beams were most suitable for resin milling (Figure 2). Large, high-quality cross-sections (> 90 µm width) of the cells could be achieved rapidly for posterior EDS analysis. TEM of resign embedded cell sections also showed that PM located inside and outside the cells.

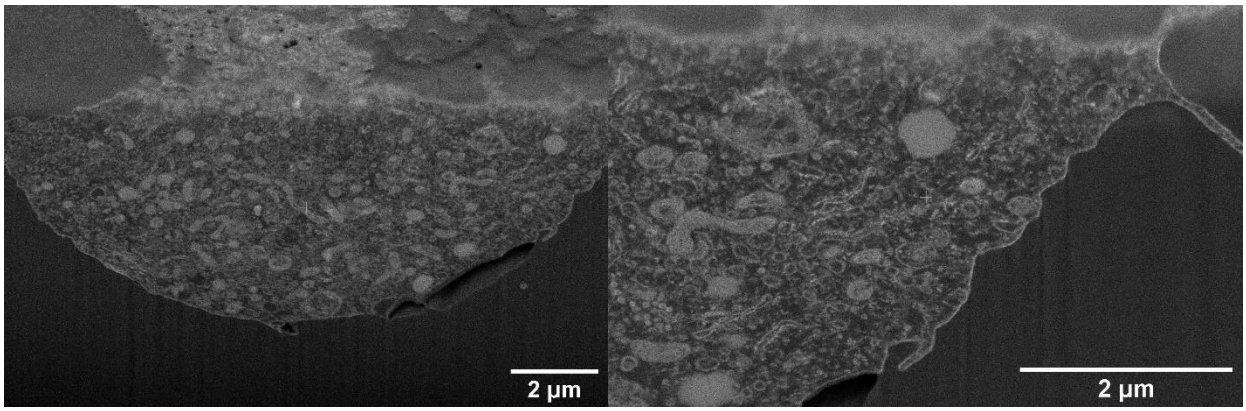

Figure 2. Oxygen Plasma FIB cross-section of embedded cells (FEI Hydra PFIB, BSE, 2kV). Cross-sectional cell area shows high contrast and resolution of stained cell organelles. This method could be used for TEM lamella preparation or 3D reconstruction of large volumes of intracellular regions of interest.

Finally, we used Soft X-ray tomography (cryo-SXT) with super resolution fluorescence structured illumination microscopy (cryo-SIM), performed in B24 beamline (DLS) to characterise cells exposed to PM [2]. The aim was to correlate between markers of oxidative stress (by fluorescence), the location of PM inside the cells and damage to the mitochondria (measured by SXT). During cryo-SIM fluorescence imaging it was observed that oxidative stress response after PM pollution exposure was variable among the cell population, and the SXT tomography assisted in understanding the cause of this variability by correlating with mitochondria structure and PM presence within the cell.

To this end, it was necessary to develop a workflow that bridges multiple length scales - from fluorescence microscopy (µm/mm-length scale) to understand the biological response of stressed cells, to the ultrastructural changes of cell organelles and PM location (nm-length scale). Introducing the 3D imaging capabilities of B24 at the front of the pipeline, together with subsequent imaging and analysis experiments, helped to understand the variability of cell damage by PM and which sizes and chemistries were responsible for causing more intracellular damage. The relevance of achieving this correlation will have an impact on identifying the most harmful PM sources and will help create mitigating and therapeutic strategies to reduce human exposure. Furthermore, moving towards all-cryo correlative experiments of the same cell cultures, will generate more rapid and reliable information of biological/inorganic materials interactions in their near-native, hydrated state [3].

https://doi.org/10.1017/S1431927622005396 Published online by Cambridge University Press

References:

[1] Hempel, C. (2017). *Apmis* **125**, 650–654. http://doi.wiley.com/10.1111/apm.12699.

[2] Kounatidis, I., et al. (2020). *Cell* **182**, 515-530.e17. http://dx.doi.org/10.1016/j.cell.2020.05.051.

[3] The authors acknowledge funding from EPSRC (CDT in the Advance Characterisation of Materials and EP/T003189/1 grant).